Journal of Groundwater Science and Engineering
ISSN 2305-7068
Indexed by ESCI CABI CSA
Scopus GeoRef AJ CNKI

**Application of GIS based analytical hierarchy process and multicriteria decision analysis methods to identify groundwater potential zones in Jedeb Watershed, Ethiopia**

Temesgen Mekuriaw Manderso, Yitbarek Andualem Mekonnen, Tadege Aragaw Worku

Citation:
Manderso TM, Mekonnen YA, Worku TA. 2023. Application of GIS based analytical hierarchy process and multicriteria decision analysis methods to identify groundwater potential zones in Jedeb Watershed, Ethiopia. Journal of Groundwater Science and Engineering, 11(3): 221-236.

View online: https://doi.org/10.26599/JGSE.2023.9280019

Journal homepage: http://gwse.iheg.org.cn

Research Paper

# Application of GIS based analytical hierarchy process and multicriteria decision analysis methods to identify groundwater potential zones in Jedeb Watershed, Ethiopia

Temesgen Mekuriaw Manderso[1*], Yitbarek Andualem Mekonnen[1], Tadege Aragaw Worku[1]

[1] *Department of Hydraulic and Water Resources Engineering, Debre Tabor University, Debre Tabor Ethiopia.*

**Abstract:** The hydrogeological situation of the study area requires the identification of groundwater potential. Remote sensing and satellite data have proven to be reliable tools for understanding various factors that affect groundwater occurrence and movement. This study employed weighted overlay analysis based on satellite imagery and secondary data to create a thematic map for characterizing groundwater potentials in the study area located within Abbay Basin, Ethiopia. Remote sensing (RS) and GIS-based Fuzzy-Analytical Hierarchy Process methods were utilized to classify groundwater potential (GWP) zones into five categories: Very good, good, moderate, poor, and very poor. The central and eastern parts of the study area were identified as having high (33.186%) and very high (2.351%) groundwater potentials, while the western part exhibited poor and very poor potential areas. The groundwater potential map delineated higher and moderate potentials, suitable for installing shallow and production bores. This research demonstrates the effectiveness of RS and GIS techniques for delineating groundwater potential zones, which can aid in the planning and management of groundwater resources. The research findings have the potential to contribute to the formulation of improved groundwater management programs in the study area.

**Keywords:** Analytical Hierarchy Process; Delineation; Groundwater potential zones; Jedeb Watershed; Remote sensing

Received: 11 Sep 2022/ Accepted: 05 Jun 2023/ Published: 15 Sep 2023

## Introduction

Groundwater, contained in subsurface geological formations, is among the most vital natural resources on Earth. It plays a crucial role in the hydrological cycle and influence essential geochemical processes beneath the soil surface (Ettazarini and El Jakani, 2020). Groundwater serves as a lifeline for numerous communities, supporting industrial development, influencing agricultural activities, and maintaining a healthy ecological balance (Ajay Kumar et al. 2020; Berhanu and Hatiye, 2020; Fildes et al. 2020; Haque et al. 2020). Effective groundwater management and sustainability primarily revolve around the responsible extraction of groundwater resources (Abudeif et al. 2015; Adeyeye et al. 2019; Atmaja et al. 2019; Haque et al. 2020; Rajasekhar et al. 2019; Yeh et al. 2016).

The delineation of groundwater potential (GWP) zones can be achieved through various methods, including statistical approaches, expert evaluation, geophysical techniques, deterministic and hydrogeological methods, as well as drilling, GIS and remote sensing techniques (Arya et al. 2020; Atmaja et al. 2019; Rajasekhar et al. 2019; Biswas et al. 2020). However, many groundwater potential investigation approaches, such as geophysical methods, ground-based surveys, and exploratory

*Corresponding author: Temesgen Mekuriaw Manderso, *E-mail address*: tmekuriaw1485@gmail.com

DOI: 10.26599/JGSE.2023.9280019

Manderso TM, Mekonnen YA, Worku TA. 2023. Application of GIS based analytical hierarchy process and multicriteria decision analysis methods to identify groundwater potential zones in Jedeb Watershed, Ethiopia. Journal of Groundwater Science and Engineering, 11(3): 221-236.

drilling, are both expensive and time-consuming, often requiring extensive data sets (Saranya and Saravanan, 2020; Biswas et al. 2020). The identification of groundwater potential zones holds particular importance in the groundwater conservation and efficient implementation of groundwater management strategies, such as determining optimal locations for drilling wells to meet various requirements for the resources such as household and irrigation needs (Ajay Kumar et al. 2020).

In recent years, several methods have been developed to delineate groundwater potential zones in various river basins. These methods involve the application of multi-criteria decision analysis (MCDA), remote sensing, GIS, and analytical hierarchical process (AHP) approaches (Das et al. 2019; Kassahun and Mohamed, 2018; Teja and Singh, 2019; Das and Pardeshi, 2018). Geospatial and remote sensing techniques play an important role in groundwater exploration, conservation, evaluation, and regional assessment, which enables the identification of diverse ground surface properties (Kavidha and Elangovan, 2012; Suryabhagavan, 2017). The integration of satellite imagery and remotely sensed data allow for a comprehensive assessment of groundwater occurrence and movement in relation to geology, geomorphology, soils, land use and land cover, drainage, and lineaments (Thapa et al. 2018). These variables are extremely important in groundwater potential modeling.

Jedeb watershed is one of the tributaries of the Abay River and serves as vital water sources for several urban areas, including Debre Markos, Erebu Gebiya, Amanual and Debre Elias towns. Several groundwater investigations have been conducted by various investigators/geologists in the Sentra well field area of the Jeded watershed, utilizing electrical resistivity survey techniques to explore groundwater resources. However, these methods are known to be time-consuming, costly, and often require specialized expertise. To overcome these limitations and facilitate groundwater exploration in this study area, this research adopts an integrated approach using GIS and remote sensing techniques. The approach provides a robust platform for the analysis of extensive data sets and supports effective decision-making processes (Ajay Kumar et al. 2020; Biswas et al. 2020; Ettazarini and El Jakani, 2020).

The primary objective of this study is to employ GIS-based Fuzzy-Analytical Hierarchy Process and Multicriteria Decision Analysis Methods to identify groundwater potential zones in the Jedeb watershed.

## 1 Study area

The Jedeb watershed is situated in the Abbay basin, with latitude and longitude ranging from 10°19′ to 10°40′ N and 37°20′ to 37°50′ E, respectively (Fig. 1). It is a significant tributary of the Abbay River, originating from the high mountain (Choke) in the northeast and flowing towards the southwest, ultimately joining the Blue Nile River at an elevation of 3 996 m.a.s.l. The watershed encompasses an area of 866.2 km$^2$ and is located northwest of Debre Markos Town, approximately 302 km from Addis Ababa. The rainy season in the Jedeb watershed typically

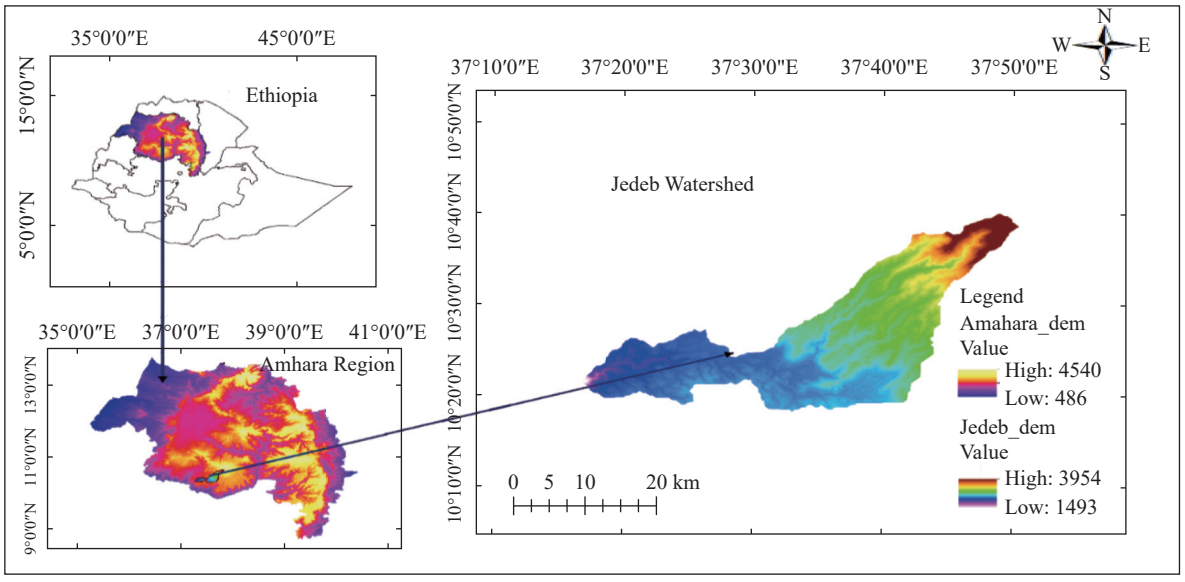


**Fig. 1** Location of study area

occurs from June to September, while the driest period usually spans from January and March, with the remaining months experiencing light rainfall. On average, the annual minimum and maximum temperatures in the area are 10.44°C and 24.27°C, respectively.

## 2 Materials and methods

### 2.1 Data collection

As stated in the objectives, this study utilize various datasets to create a comprehensive database for delineating groundwater potential. These datasets include remote sensing-based products, meteorological, hydrological data, geological data, topographical data, and soil data. Satellite remote sensing provides a reliable and valuable tool to generate accurate data for groundwater exploration. It helps reduce the time and cost associated with traditional geological and geophysical fieldwork prospecting in groundwater exploration.

To create a slope and drainage density maps, a digital elevation model (DEM) with a resolution of 12.5 m was obtained from the Shuttle Radar Topography Mission (SRTM). ArcGIS tools were used for the processes such as sink filling, flow direction, flow accumulation, and stream network extraction. The drainage density map was generated using the line density method. The lineament density and land use/land cover (LULC) maps were created using a Landsat 8 Operational Land Imager (OLI) satellite image obtained from the USGS website. The line module of PCI Geomatica 2018 was employed for automatic lineament extraction.

For rainfall mapping the Kriging method was applied, while the Harmonized World Soil Database (HWSD) was utilized to generate a soil map of the research area.

#### 2.1.1 Data preparation and identification of factors influencing groundwater occurrence

The occurrence and flow of groundwater are influenced by various factors that include geology, geomorphology, soil, drainage density, lineament density, surface water body, land cover, slope, rainfall, and others. The selection of these factors as indicators primarily depends on the specific goals of the study. For instance, in their research, Teja and Singh (2019) utilized eight parameters to assess groundwater potential zones; these factors included rainfall, soil pattern, slope, land use and land cover, drainage density, lineaments, geology, and geomorphology. It is worth noting that the relative importance and influence of these factors mayvary depending on the specific context and location under consideration. In the field of spatial science, data are collected from different sources which are often in varying formats and resolutions, necessitating the harmonization of data into a uniform format and resolution (Savita et al. 2018). Consequently, the data processing task involves in pre-processing and post-processing activities.

#### 2.1.2 Rainfall

In the water cycle, rainfall is one of the most important sources of groundwater recharge. However, rainfall distribution varies across different locations due to variations in environmental conditions. High levels of rainfall indicate a greater potential for groundwater recharge, while lower levels suggest lower recharge potential. Consequently, areas experiencing abundant rainfall are associated with high groundwater potential zones. To assess the average yearly rainfall, data from each monitoring station spanning a period of 30 years were considered. Since mean annual rainfall is typically point data specific to each station, it can be transformed into continuous spatial data using ordinary kriging interpolation method on the GIS environment.

#### 2.1.3 Soil media

Soil plays a crucial role in determining the availability of groundwater. The study of soil helps to identify its types and properties, which are essential in understanding groundwater dynamics. The porosity and permeability of soil significantly impact the movement of groundwater and the infiltration of surface water into aquifer system. Therefore, conducting soill investigation is necessary to assess the groundwater potential in specific locations. The soil properties have a direct influence on the relationship between runoff and infiltration rates, which in turn control the degree of permeability. Permeability is a fundamental factor in hydrogeology, as it governs both quantity and quality of groundwater (Sivakumar, 2019).

#### 2.1.4 Slope

Slope is an important factor to consider when assessing groundwater potential zones and risk areas. The slope (in degrees) of the study area will be calculated using a digital elevation model (DEM) obtain from the SRTM. In general, flat regions tend to retain water for longer periods, allowing for increased water penetration or recharge and potentially higher risk of pollutant transport. Steep slopes, on the other hand, tend to have higher runoff and lower infiltration. Consequently, steep slopes are assigned lower ratings, while flat

areas receive higher ratings (Hammouri et al. 2012; Gelagay and Minale, 2016; Teja and Singh, 2019). Among the variables, topography has the least impact. However, the degree of slope, which varies across different areas, controls the likelihood of rainfall runoff or retention long enough for infiltration (Abdalla et al. 2020; Janarthanan and Thirukumaran, 2020). Therefore, the slope of Jedeb watershed that represents topography will be reclassified and analyzed in this study.

#### 2.1.5 Land use and Land cover (LU/LC)

The Landsat 8 sensors were utilized to acquire the necessary imagery for this study. A total of seven bands with a spatial resolution of 10 meters were extracted from the images. The research area was then subset from the acquired data after loading the images into ERDAS IMAGINE 2014 software. The primary goal of this stage was to perform satellite data analysis and interpretation in order to create a thematic map of land use/land cover. The digital images underwent various processing procedures, including pre-processing, categorization, and accuracy evaluation, following established protocols (Deepa et al. 2016).

#### 2.1.6 Drainage density

Drainage density refers to the spacing of stream channels, indicating the permeability of the rock, the rate of infiltration, and recharge processess (Allafta and Opp, 2021; Jabbar et al. 2019). It provides insights into the relative balance between precipitation infiltration and surface runoff. In areas where rocks are highly permeable, infiltration into groundwater is more significant, resulting in reduced surface water runoff. In contrast, in regions with low permeability rocks, there is less infiltration and greater. Therefore, lower drainage density is typically associated with increased recharge potential and higher groundwater potential (Takorabt et al. 2018).

$$DD = \frac{\sum L_i}{A} \quad (1)$$

#### 2.1.7 Lineament density

Lineaments are linear geomorphologic structures present in the Earth's crust that indicate zones of weakness or structural displacement at the surface. These lineaments, such as faults, often correspond to areas of fracturing and enhanced secondary porosity and permeability, which can contribute to increased groundwater occurrence and movement (Abdalla et al. 2020; Kindie et al. 2019). In hard rock terrain, the presence of lineaments and fissures that create secondary porosity, play a crucial role in regulating the flow and storage of groundwater. The lineament characteristics of the study area were derived from a lithology map using digitization technique in GIS, and the lineament map was prepared. Using kernel density analysis tool in the GIS software, the lineament density of the study region was estimated and classified.

$$LD = \frac{\sum L_i}{A} \quad (2)$$

#### 2.1.8 Geology

The significance of geologic units in relation to groundwater occurrence was assessed by considering various characteristics, including rock type and thickness, fracture density, compactness, and the type and degree of cementation. The importance of each factor was determined on the basis of its impact on groundwater dynamics and behavior (Saha et al. 2018).

#### 2.1.9 Geomorphology

Geomorphology involves the study of landforms and structural elements, such as hills, plateaus, pediments, alluvial, and rift floors, to have a better understanding of hydrological characteristics within a particular region (Shadeed et al. 2019; Ikegwuonu et al. 2021; Province et al. 2021). Geomorphological investigations play a vital role in assessing water resources, including both surface water and groundwater, within the study area. Geomorphological mapping entails the identification and classification of diverse landforms and structural elements that influence the occurrence groundwater (Gelagay and Minale, 2016).

### 2.2 Identification of groundwater potential using a GIS-based fuzzy-AHP

The potential zones and appropriate groundwater recharge sites were identified by employing a combined approach using remote sensing (RS) and geographic information system (GIS) techniques based on multi-criteria decision analysis (MCDA) approaches and fuzzy Analytical Hierarchy Process (AHP) (Duan et al. 2016). The fuzzy AHP is particularly valuable for addressing complex decision-making in the field of groundwater (Arulbalaji et al. 2019). This approach simplifies complex judgments by transforming them into a series of pair-wise comparisons and synthesizing the results. Additionally, the fuzzy AHP tool effectively assess the consistency of a result, thereby reducing bias in the decision-making process (Pande et al. 2021; Sivakumar, 2019). To facilitate analysis, the maps are converted to raster format and appropriate weights are assigned to them based on their rank in groundwater poten-

tiality (Shao et al. 2020).

To compare all of the theme levels, a pair-wise comparison matrix was constructed. The assigned weights' consistency index (*CI*) was determined using the approach recommended by Saaty. Additionally, the consistency ratio (*CR*), which indicates the likelihood that the matrix ratings were generated randomly, was calculated using the values of the random consistency index (*RI*). The RI is the average value of *CI* for random matrices based on the Saaty scale.

$$CI = \lambda_{\max} - n/n - 1 \quad (3)$$

Where: $n$ is the number of criteria or elements being considered.

The formula for calculating the consistency ratio is as follows:

$$CR = \frac{CI}{RI} \quad (4)$$

It is important to note that consistent weights should have a *CR* value of less than 0.10; otherwise, associated weights must be re-evaluated to minimize inconsistencies (Saaty, 1992).

After the categorization process, a GIS model will be used to derive groundwater potential zones suitable for exploration using a weighted overlay technique. This involves multiplying the scale value of each reclassified layer (parameter) by its assigned weight, resulting in the calculation of groundwater potential values for each cell in the study area. The final output raster will consist of these cell values, providing an indication of potential groundwater areas. The relative importance of each groundwater governing parameter and the respective classes that each feature belongs are examined using the following Equation (5):

$$\mathrm{GWPZ} = \sum W_i * \mathrm{G} + W_i * \mathrm{Ge} + W_i * \mathrm{Dd} + W_i * \mathrm{Ld} + W_i * \mathrm{So} + W_i * \mathrm{Sl} + W_i * \mathrm{LULC} + W_i * \mathrm{R} \quad (5)$$

Where: GWPZ represents groundwater potential zonation, G denotes geology, Ge refers to geomorphology, R represents rainfall, Ld indicates lineament density, So is the soil type, Dd stands for drainage density and LULC for land use/ land cover, and Sl represents slope.

By applying this equation, the method evaluates the relative importance of each groundwater governing parameter and the respective classes associated with them.

## 3 Result and discussions

Each class within the eight thematic layers, including slope, lineament density, rainfall, geomorphology, geology, soil, land use/cover, and drainage density, is qualitatively categorized into five potential zones: Very good, good, moderate, moderate to poor, and very poor. These categories are determined based on the contribution of each class to groundwater potential in the study area. The reclassified thematic layer assigns a lower value to the class with a lesser contribution to groundwater potential, and a higher value to the class with a greater contribution. The distinct eight classes have been assigned appropriate values based on their behavior in terms of controlling groundwater potentialand their relative importance to other classes.

### 3.1 Interpretation of thematic maps

#### 3.1.1 Drainage density

Drainage density is a measure of the total length of all stream segments per unit area, which represents the proximity of stream channels in a given area (Teja and Singh, 2019). In areas where the lithology is primarily massive, the ability of ground to absorb and percolate rainfall decreases. Consequently, a significant portion of precipitation forms runoff on the surface. In the studied catchment, the drainage density is calculated to be 1.59531 km/km$^2$. Locations with extremely high drainage density (3.35579–6.8458) typically exhibit weak groundwater potential. Conversely, areas with very low drainage density (0.0–0.698) allow for greater infiltration and recharge of groundwater, thereby demonstrating higher potential for groundwater occurrence, particularly in downstream areas of the study region. In the reclassified map shown in Fig. 3 and Table 2, higher values indicate greater drainage density, which favors runoff. The higher rate values in the reclassified map (Fig. 3b) indicate the greater potential for groundwater infiltration.

#### 3.1.2 Slope

The gradient of slope has a direct impact on the infiltration of rainfall by affecting runoff speed, runoff retention in the subsurface, and the infiltration capacity. On steep slopes, water flows

**Table 1** Different values of N, Saaty's ratio index (Abdalla et al. 2020; Allafta and Opp, 2021; Jabbar et al. 2019; Savita et al. 2018; Teja and Singh, 2019)

| N | 1 | 2 | 3 | 4 | 5 | 6 | 7 | 8 | 9 | 10 | 11 | 12 |
|---|---|---|---|---|---|---|---|---|---|---|---|---|
| RI | 0.00 | 0.00 | 0.58 | 0.90 | 1.12 | 1.24 | 1.32 | 1.41 | 1.45 | 1.49 | 1.51 | 1.48 |

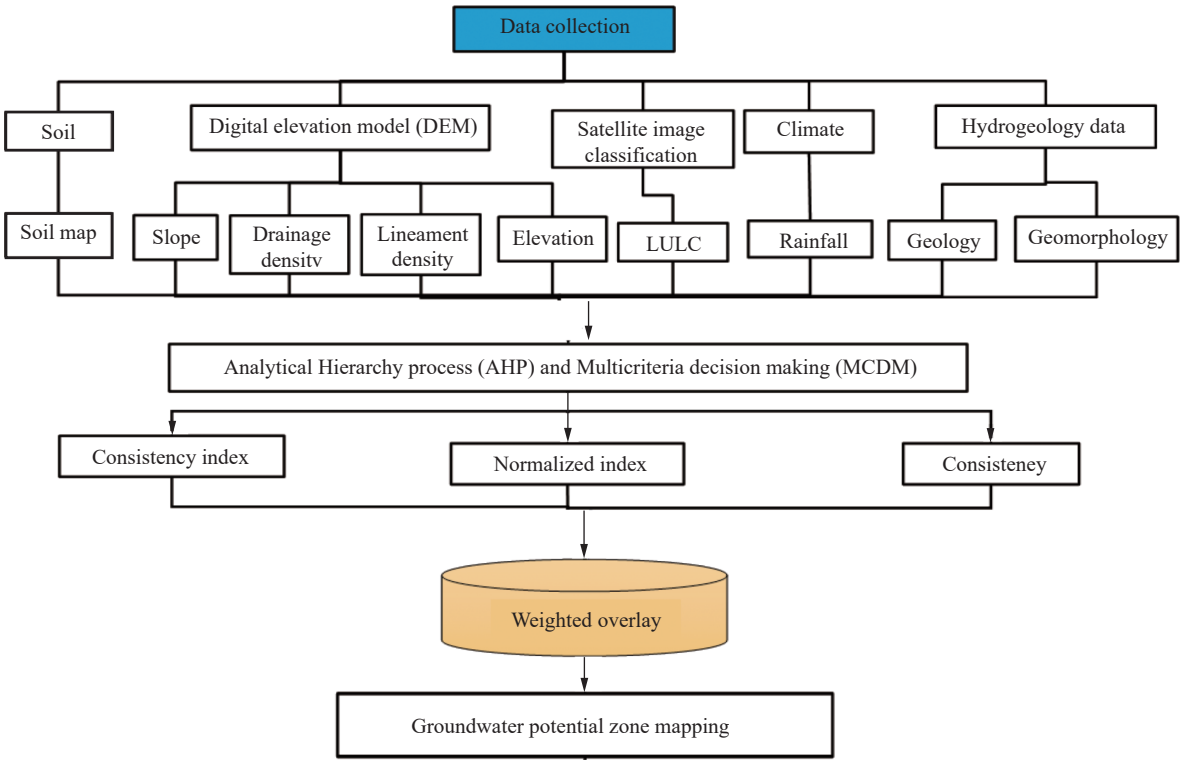


**Fig. 2** Work flow

rapidly during rainfall events, leaving insufficient time to rainwater infiltration and groundwater recharge. As a result, larger slopes usually yield lower recharge potential. In contrast, gentle slope areas allow for slower surface runoff, providing rainwater with longer period for percolation and infiltration. As shown in Table 3, the slope percentage in the study region varies from 0 to 69.885% and has been categorized into five groups. Slopes ranging from 0 to 4.272% approximately covered 19.23% of the research area (166.5 km$^2$), indicating excellent groundwater potential

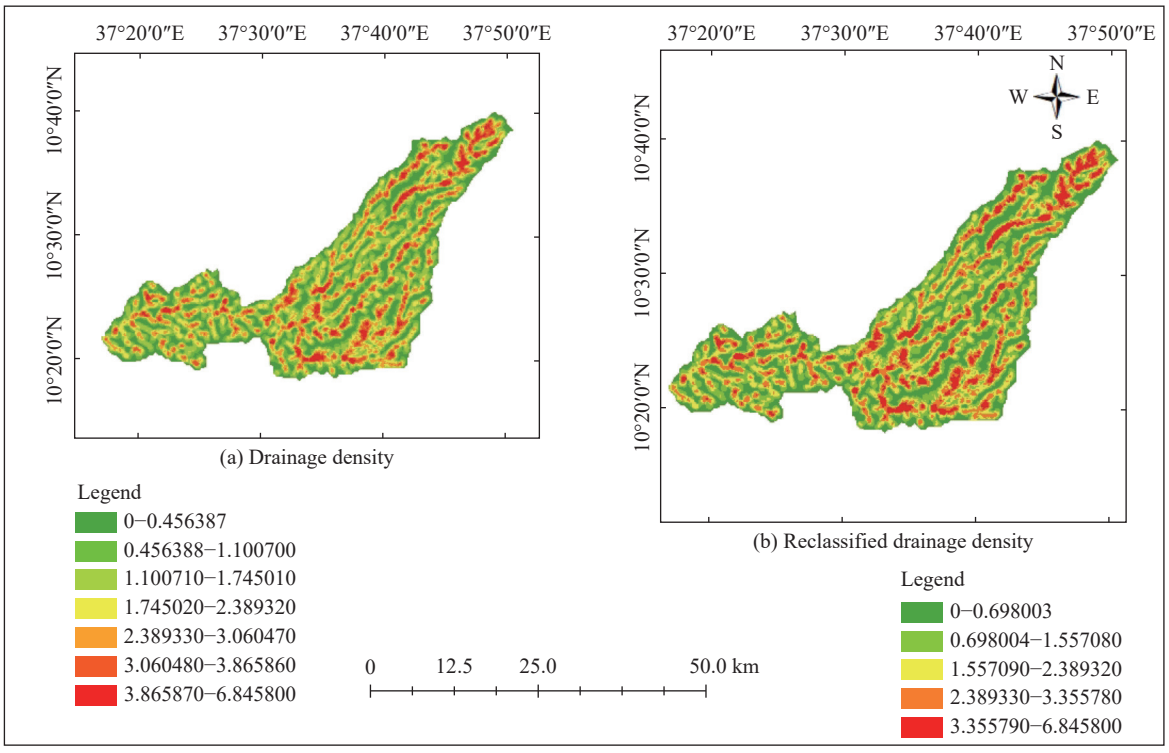


**Fig. 3** Drainage density a) before reclassification b) after reclassification

**Table 2** Rate and ranks of drainage density

| Drainage density / km/km$^2$ | Rank | Area / km$^2$ | Percent / % |
|---|---|---|---|
| 0–0.698 | Very low | 23.103 | 26.659 |
| 0.698–1.56 | Low | 22.500 | 25.963 |
| 1.56–2.39 | Moderate | 19.591 | 22.606 |
| 2.39–3.36 | High | 151.453 | 17.476 |
| 3.36–6.858 | Very high | 63.240 | 7.297 |

due to reduced runoff and longer residence time for infiltration. In the mild slope category of 4.272%–8.312 24%, the areas of approximately 266.69 km$^2$ (30.77% of the study area) are considered to have good groundwater occurrence. The area (284.40 km$^2$) with slopes of 8.312%–15.672% is assumed to have moderate potential for groundwater. The areas with steep slopes in a range of 15.6717%–30.5708% are classified as having poor groundwater potential, while the areas (133.67 km$^2$) with very steep slopes ranging from 30.5709% to 69.865% are categorized as very poor groundwater potential zone. In summary, smaller slope values correspond to flatter terrain with a gentle slope, indicating more favorable conditions for groundwater potential; whereas larger slope values correspond to steeper terrain with sharp slopes, indicating reduced groundwater potential.

### 3.1.3 Geomorphology

The research region comprises various geomorphic units, including residual deposit, alluvial deposit,

**Table 3** Rank and rate of slope layer

| Slope in degrees | Condition | Rank | Area / km$^2$ | Percent / % |
|---|---|---|---|---|
| 0–4.272 | Flat | Very Good | 166.65 | 19.23 |
| 4.272–8.312 2 | Gentle | Good | 266.69 | 30.77 |
| 8.312–15.672 | Medium | Moderate | 284.40 | 32.82 |
| 15.672–30.571 | Steep | Poor | 133.67 | 15.42 |
| 30.571–69.865 | Highly steep | Very poor | 15.23 | 1.76 |

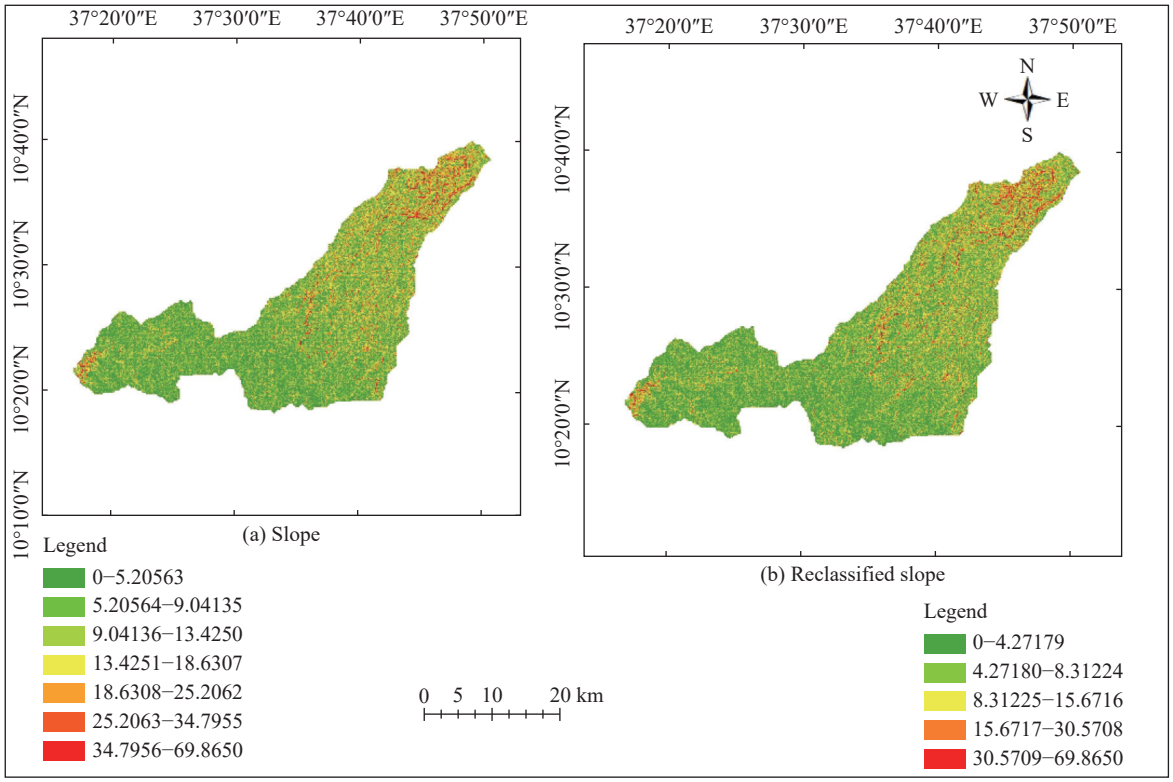


**Fig. 4** Slope a) before reclassification b) after reclassification

and volcanic landforms, as shown in Table 4 and Fig. 5. Among them, the residual deposits cover an area of approximately 3 053.38 km$^2$ (79.73%) and are deemed to be extremely favorable for groundwater potential, as indicated in Table 4. Alluvial deposits occupy an area of 253 km$^2$ (6.61%) and are considered as having groundwater potential. Volcanic landforms cover 522.41 km$^2$ (13.64%) and are classified as the poor for groundwater potential zone. As illustrated in Fig. 5, higher reclassified values and rates indicate a relatively good contribution of the respective geomorphic units to groundwater potential.

#### 3.1.4 Geology

The types of geology present at the surface have a significant influence on the percolation and flow of water through the soil, thereby influencing groundwater recharge. Geology also plays a key role in determining the abundance and distribution of groundwater availability. Table 5 provide a comprehensive rankings of geological units in the study area, based on the understanding of their hydrostratigraphic features.

#### 3.1.5 Lineament density

The lineaments, as illustrated in Fig. 7, are surficial manifestation of geological structures, including faults, cleavages, fractures, and other geological discontinuities, that exhibit in straight or slightly curved lines and can be identified through remote sensing techniques. Table 6 shows that areas characterized by high lineament density ( ranging from 1.77 km/km$^2$ to 2.74 km/km$^2$) are regarded to have good groundwater potential. The largest lineament density is observed in the central, northwestern escarpments, and central part of the watershed, as revealed by the findings. Fig. 7 and Table 6 depict the lineament density classes ranked on the basis of their rate/rank values. The class with highest rate/rank (ranging from 1.769 km/km$^2$ to 2.735 2 km/km$^2$) receives the highest ranking,

**Table 4** Geomorphologic description and rate of the layer (FAO)

| Geomorphology | Landforms | Area / km$^2$ | Percent / % |
|---|---|---|---|
| High to mountainous relief hills | Volcanic land form | 203.229 6 | 3.66 |
| Moderately dissected plateaux, plateaux with hills abd rolling to hilly plateau | | 324.154 | 0.99 |
| Plains and low plateaux with hills, moderately dissected sideslopes and dissected plains | | 8.151 2 | 95.35 |
| Moderately dissected plateaux, plateaux with hills and rolling to hilly plateau | Residual land form | 298.872 8 | |
| Moderate to high relief hills and severely dissected side slopes and plateaux | | 0.464 8 | |
| Seasonal wetland and seasonally waterlogged land | Alluvial land form | 31.703 2 | |

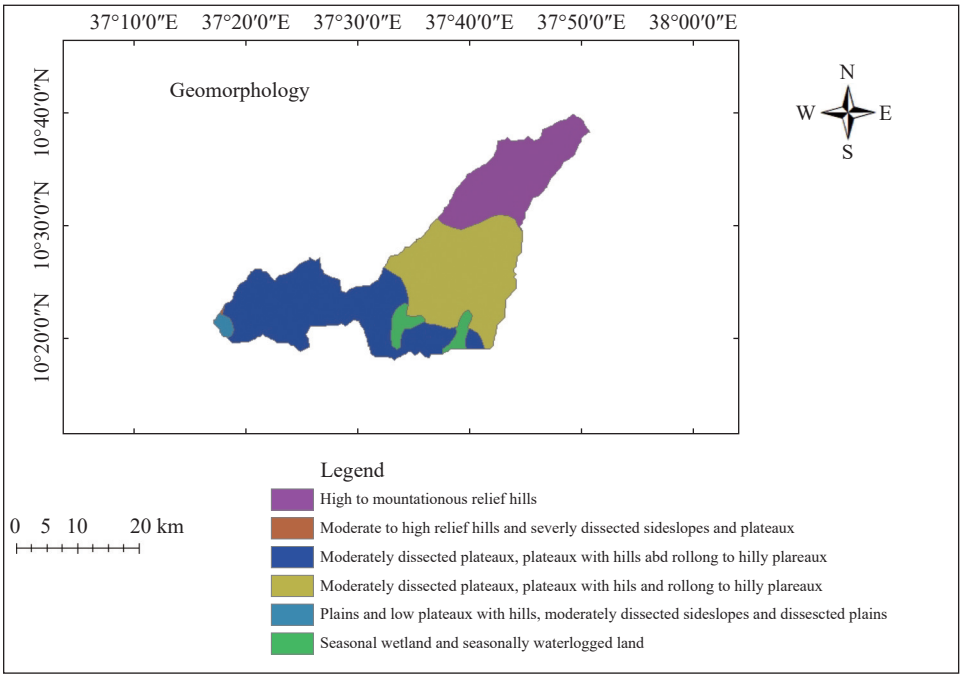


**Fig. 5** Geomorphology

**Table 5** Rank and rate of geology layer

| Geology | Rank | Area / km$^2$ | Percent / % |
|---|---|---|---|
| PreCambrian | Low | 1.048 | 0.12 |
| Cretaceous-Jurassic | Moderate | 126.86 | 14.64 |
| Tertiary extrusive and intrusive | High | 738.671 | 85.24 |

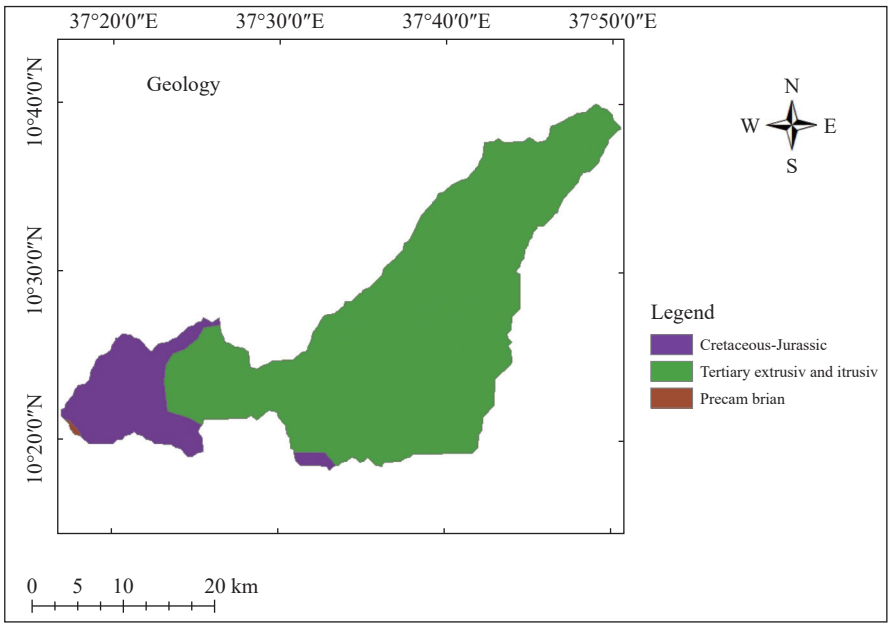


**Fig. 6** Geology of the study area

while the class with the lowest rate/rank (ranging from 0 km/km$^2$ to 0.3218 km/km$^2$) received the lowest ranking.

### 3.1.6 Rainfall

Rainfall is plays a significant role in influencing groundwater recharge. In the Jedeb watershed, rainfall is categorized into five groups using equal interval classification method based on the annual rainfall data from 2020. Fig. 8 and Table 7 illustrate the classified rainfall map and the

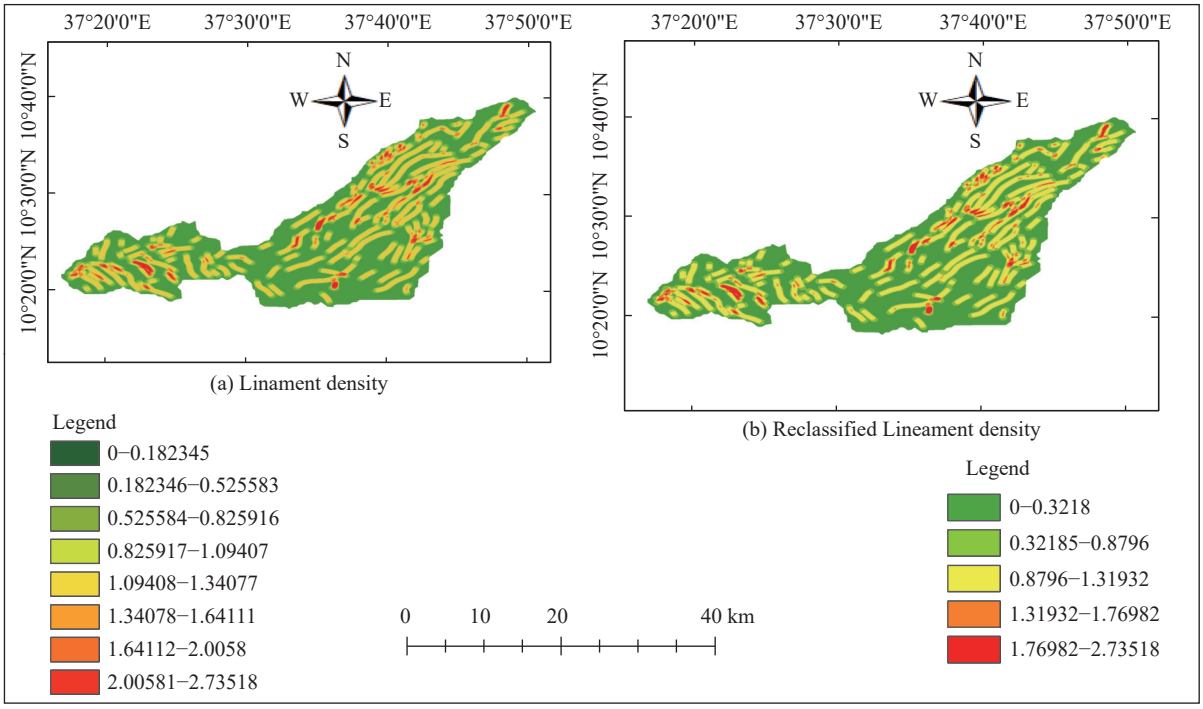


**Fig. 7** Lineament density a) before reclassification b) after reclassification

**Table 6** Rate and rank of lineament density theme

| Lineament density / km/km$^2$ | Rank | Area / km$^2$ | Percent / % |
|---|---|---|---|
| 0–0.322 | Very low | 439.341 | 50.695 |
| 0.32185–0.88 | Low | 146.745 | 16.933 |
| 0.88–1.32 | Moderate | 235.726 | 27.200 |
| 1.32–1.77 | High | 29.220 | 3.372 |
| 1.77–2.74 | Very high | 15.603 | 1.800 |

corresponding rates. The study area's rainfall map was generated by interpolating the mean annual rainfall data obtained from the CHRS portal using kriging interpolation. Table 7 shows the average annual rainfall in the area, ranging from 1 190 mm to 1 640 mm. In general, a higher yearly rainfall indicates the presence of considerable groundwater potential, which can vary based on factors such as the rock type and slope.

### 3.1.7 Land use and land cover

Land use/land cover has an significant impact on runoff, as it can either promote the movement of water or retain it on the surface. The type of vegetation or cover on the land surface influences the roughness, which in turn affects percolation of water. Fig. 9 and Table 8 depict the land use/land cover distribution in the research area, including categories such as barren ground, settlement, cultivated land, shrubland and grassland, forest, and water bodies. In the Jedeb watershed, agricultural land covers the largest extent, encompassing approximately 642.777 km$^2$. Settlement areas occupy 122.838 km$^2$, while grassland, shrubland, forest, water bodies, and barren land cover an area of 29.571 km$^2$, 26.674 km$^2$, 43.785 km$^2$, 0.797 km$^2$ and 0.181km$^2$, respectively. Among them, barren land and settlement tend to have very poor groundwater potential due to their low infiltration capacity. Conversely, water body, shrubland, grasslands, agricultural land, and forested areas are considered to have varying degrees of very good, moderate, and high groundwater potential.

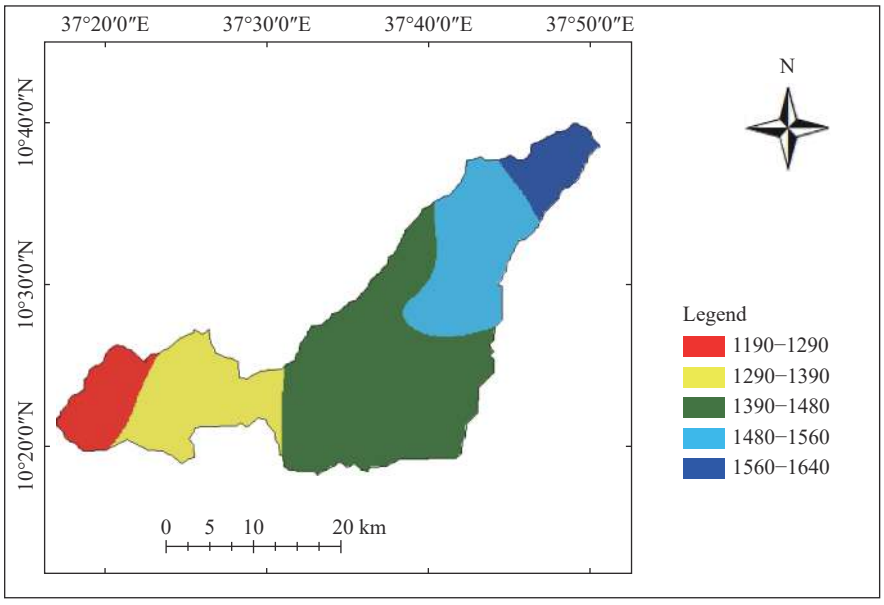


**Fig. 8** Annual mean rainfall distribution

**Table 7** Rate and ranks of RF layer

| Rainfall / mm | Rank | Area / km$^2$ | Percent / % |
|---|---|---|---|
| 1 190–1 280 | Very Poor | 75.575 | 8.721 |
| 1 280–1 370 | Poor | 151.312 | 17.460 |
| 1 380–1 460 | Moderate | 403.333 | 46.540 |
| 1 460–1 550 | Good | 178.135 | 20.555 |
| 1 550–1 640 | Very good | 58.275 | 6.724 |

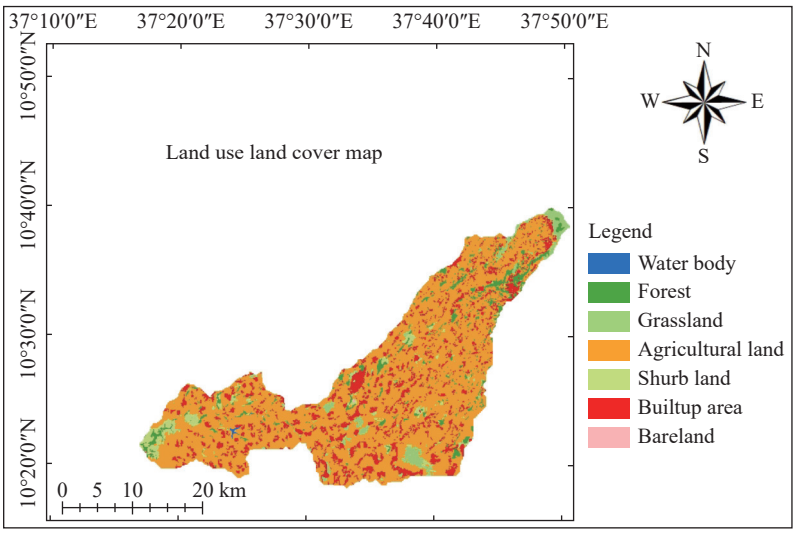


**Fig. 9** Land use land cover

**Table 8** Area coverage and rate of LU/LC

| Land use type | Rank | Area / km$^2$ | Percent / % |
|---|---|---|---|
| Water body | Very high | 0.797 | 0.092 |
| Forest | High | 43.785 | 5.052 |
| Grassland | Moderate | 29.571 | 3.412 |
| Agricultural land | Moderate | 642.777 | 74.170 |
| Shurbland | Moderate | 26.674 | 3.078 |
| Builtup Area | Very poor | 122.838 | 14.174 |
| Bareland | Very Poor | 0.181 | 0.021 |

#### 3.1.8 Soil types

Soil characteristics play a crucial role in controlling the penetration of surface water into the groundwater system. These characteristics directly influence the rates of infiltration, percolation, and permeability, and water retention and infiltration capacity of the soil. In the study area, the predominant soil categories include luvisols, Nitosols, and Vertisols, as shown in Table 9 and Fig. 10.

## 3.2 Thematic layer integration and groundwater potential zone mapping

As discussed later in this section, all thematic layers have a consistency ratio (*CR*) of less than 0.1, indicating reasonable pair-wise comparison judgments within each thematic layer (Table 10). For the delineation of groundwater potential zones, a weighted index overlay analysis approach was

**Table 9** Soil type rank and rate

| Soil type | Soil group | Area / km$^2$ | Percent / % | Ranks |
|---|---|---|---|---|
| Chromic Cambisols | Cambisols | 29.9648 | 3.46 | |
| Chromic Luvisols | Luvisols | 112.8032 | 13.02 | Moderate |
| Chromic Vertisols | Vertisols | 92.0356 | 10.62 | Poor |
| Dystric Nitosols | Nitosols | 3.6436 | 0.42 | Very high |
| Eutric Fluvisols | Fluvisols | 0.5336 | 0.06 | Very high |
| Eutric Nitosols | Nitosols | 138.4196 | 15.97 | Very high |
| Lithosols | Lithosols | 19.082 | 2.20 | High |
| Orthic Acrisols | Acrisols | 4.4128 | 0.51 | Poor |
| Pellic Vertisols | Vertisols | 465.6804 | 53.74 | Poor |

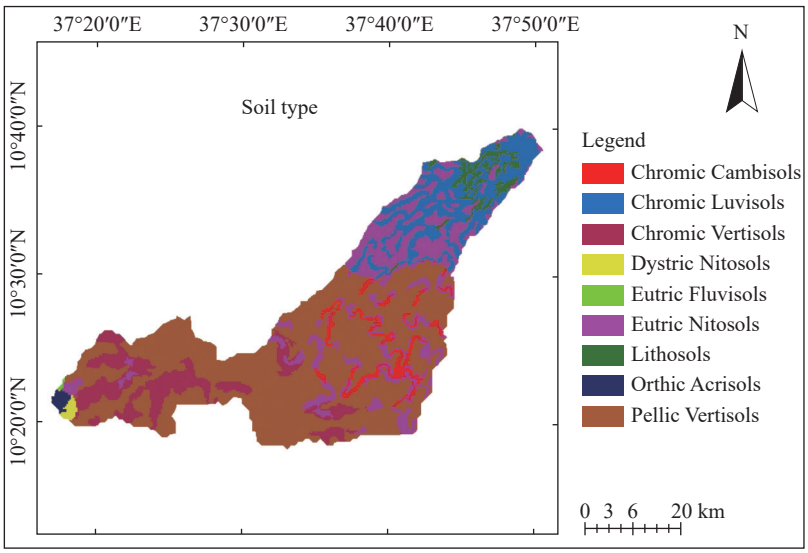


**Fig. 10** Soil type distribution map

used, successfully delineating the potential zones, as illustrated in Fig. 11. Thematic maps of geology, geomorphology, soil, slope, land use/land cover, rainfall, lineament density, and drainage density were integrated to identify and delineate groundwater potential zones in the Jedeb watershed.

**Table 10** The relative weight of each thematic layers

| Matrix | R | Ge | Sl | Geom | Dd | LULC | Ld | S | Weight / % |
|---|---|---|---|---|---|---|---|---|---|
| R | 1 | 3 | 3 | 3 | 5 | 5 | 5 | 7 | 33.09 |
| Ge | 0.33 | 1 | 3 | 1 | 3 | 5 | 5 | 5 | 20.39 |
| Sl | 0.33 | 0.33 | 1 | 3 | 1 | 3 | 3 | 5 | 13.97 |
| Geom | 0.33 | 1 | 0.33 | 1 | 1 | 2 | 5 | 3 | 11.35 |
| Dd | 0.2 | 0.33 | 1 | 1 | 1 | 1 | 2 | 3 | 8.24 |
| LULC | 0.2 | 0.2 | 0.33 | 0.5 | 1 | 1 | 1 | 3 | 5.69 |
| Ld | 0.2 | 0.2 | 0.33 | 0.2 | 0.5 | 1 | 1 | 1 | 4.06 |
| S | 0.143 | 0.2 | 0.2 | 0.33 | 0.33 | 0.33 | 1 | 1 | 3.20 |

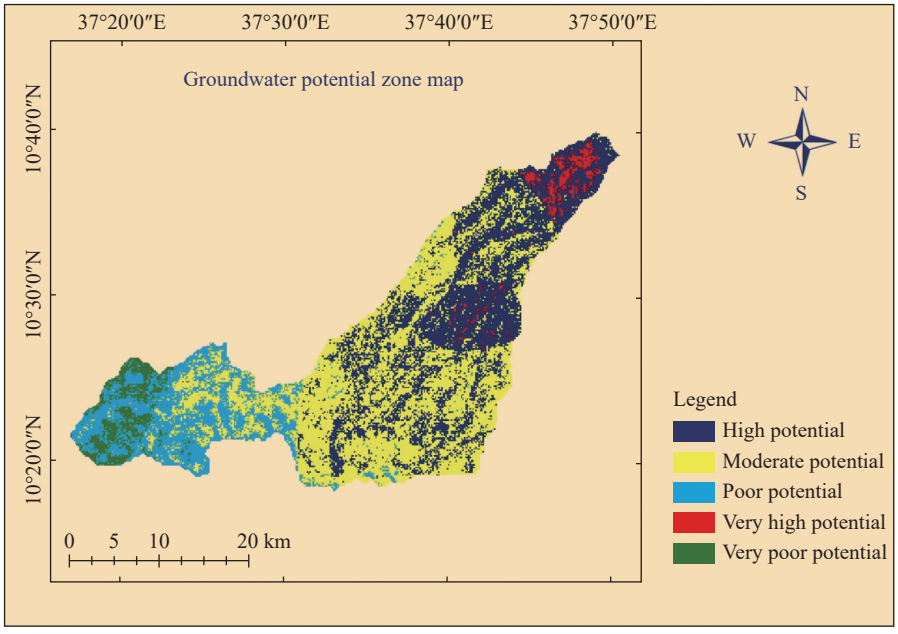


**Fig. 11** Groundwater potential zone map in Jedeb watershed

The relative impact of each factor was evaluated using the principal Eigenvector computation, from which the factor weights that reflect their influence on groundwater potential were obtained. Furthermore, the factor layers were combined using ArcGIS map algebra (raster calculator) by applying the formula (Equation 5) that is described in Equation 6. Fig. 11 and Table 11 present the classification of five groundwater potential zones: Very good, good, moderate, poor, and very poor. The high potential zones occupy the largest aerial extent of 687.027 km$^2$, followed by very good, good, and moderate zones covering 20.303 km$^2$, 286.637 km$^2$, and 380.087 km$^2$, respectively. The remaining areas, with an aerial extent of approximately 141.197 km$^2$ and 35.516 km$^2$, respectively, are classified as poor and very poor potential zones.

$$GWP = 0.33 * R + 0.204 * Ge + 0.139\,7 * Sl + 0.113\,5 * \text{Geom} + 0.082\,4 * Dd + 0.032 * S + 0.056\,9 * LULC + 0.040\,6 * Ld \quad (6)$$

Where: *GWP* stands for groundwater potential, *Sl* stands for slope, *LD* stands for lineament density, *R* stands for rainfall, *Geom* stands for geomorphology, *Ge* stands for geology, *S* stands for soil type, *LULC* stands for land use/cover, *Dd* stands for drainage density. In addition, the consistency ratio (*CR*) is calculated as follows:

$$CI = \frac{(\lambda_{\max} - n)}{(n-1)} = CI = \frac{(8.54 - 8)}{(8-1)} = 0.0771 \quad (7)$$

$$CR = \frac{CI}{RI} = \frac{0.077\,1}{1.41} = 0.05471 \quad (8)$$

Where: $RI = 1.41$ for n = 8, $\lambda_{max} = 8.540$.

So, the judgment is exactly consistent since $CR = 5.5\%$ is much less than 10%.

Where: $W_i$ is the relative weight of each thematic layers in the i$^{th}$ row.

The very good and good GWP zones are predominantly characterized by flat to moderate slope classes, high lineament density, and residual and alluvial geomorphological classes. These potential zones align with Luvisols, Nitosols and Fluvisols, Lithosols soil types and are associated with basalt formations related to the volcanic centers and alluvial plains. Areas with moderate GWP exhibit features such as gentle slope, alluvial landform, moderate rainfall, and shrubland as dominant land use/cover. The poor and very poor potential zones are located along hilly, rocky, and steep mountain terrains, all of which contribute to excessive runoff and low infiltration capacity. Areas near Choke Mountain show good GWP, while the southwestern, northern, and northeastern areas exhibit high and very high GWP. Vertisols, characterized by clay texture and massive volcanic basalts, are identified to be very poor GWP zones. Overall, the groundwater potential of the is predominantly influenced by the lithology of the terrain. Watershed areas near choke and Sentara well field exhibit higher GWP, smaller areas in the northwestern, southern, and central southern parts contribute to moderate GWP.

## 4 Conclusion

The integration of remote sensing (RS) and geographic information system (GIS) technologies have proven to be an efficient approach for groundwater potential assessment studies. By utilizing RS and GIS-based multi-criteria decision analysis (MCDA) in conjunction with available geological and borehole information, valuable insights can be gained regarding the hydrogeological conditions of an area. In the Jedeb watershed, the application of RS and GIS techniques for delineating groundwater potential zones has demonstrated its effectiveness in terms of time and cost savings, as well as enabling informed decision-making for sustainable water resource management.

Through the utilization of satellite imagery and conventional data, thematic layers representing lithology, soil type, geomorphology, lineament density, drainage density, slope, land use/cover, and rainfall were generated to create a comprehensive groundwater potential zoning map of the Jedeb watershed. On the map, groundwater potential has been classified into five categories

**Table 11** Rank and area coverage of groundwater potential zones

| Classes | Rank | Area / km$^2$ | GWP weighted area / % |
|---|---|---|---|
| 1 | Very poor potential | 35.516 | 4.112 |
| 2 | Poor potential | 141.197 | 16.347 |
| 3 | Moderate potential | 380.087 | 44.005 |
| 4 | High potential | 286.637 | 33.186 |
| 5 | Very high potential | 20.303 | 2.351 |
| Total | | 866.63 | 100 |

based on natural break classification algorithm in GIS: Very low, low, moderate, good, and very good.

Findings of the study reveal that 4.112% of the area is classified as "very poor", 16.347% as "poor", 44.005% as "moderate", 33.186% as "high", and 2.351% as "very high" groundwater potential zones. The areas with the highest groundwater potential are primarily located in severely weathered alluvial deposits with excellent permeability. Conversely, poor and extremely poor groundwater potential areas are typically found in topographical mountainous regions characterized by heavy runoff and, resulting in lower groundwater potential.

In conclusion, the integration of RS and GIS techniques has proven to be a valuable approach for assessing groundwater potential in the Jedeb watershed. The generated groundwater potential map provides essential information for sustainable water resource management and can aid in decision-making processes related to groundwater exploration and utilization.

## References


Abdalla F, Moubark K, Abdelkareem M. 2020. Groundwater potential mapping using GIS, linear weighted combination techniques and geochemical processes identification, west of the Qena area, Upper Egypt. Journal of Taibah University for Science. DOI：10.1080/16583655.2020.1822646.

Abudeif AM, Abdel Moneim AA, Farrag AF. 2015. Multicriteria decision analysis based on analytic hierarchy process in GIS environment for siting nuclear power plant in Egypt. Annals of Nuclear Energy, 75: 682−692. DOI：10.1016/j.anucene.2014.09.024.

Adeyeye OA, Ikpokonte EA, Arabi SA. 2019. GIS-based groundwater potential mapping within Dengi area, North Central Nigeria. Egyptian Journal of Remote Sensing and Space Science, 22(2): 175−181. DOI：10.1016/j.ejrs.2018.04.003.

Ajay Kumar V, Mondal NC, Ahmed S. 2020. Identification of groundwater potential zones using RS, GIS and AHP techniques: A case study in a part of Deccan Volcanic Province (DVP), Maharashtra, India. Journal of the Indian Society of Remote Sensing, 48(3): 497−511. DOI：10.1007/s12524-019-01086-3.

Allafta H, Opp C Patra S. 2021. Identification of groundwater potential zones using remote sensing and GIS techniques : A case study of the Shatt Al-Arab Basin. Remote Sensing, 13(1): 112. DOI：10.3390/rs13010112.

Arulbalaji P, Padmalal D, Sreelash K. 2019. GIS and AHP techniques based delineation of groundwater potential zones: A case study from Southern Western Ghats, India. Scientific Reports, 9(1): 1−17. DOI：10.1038/s41598-019-38567-x.

Arya S, Subramani T, Karunanidhi D. 2020. Delineation of groundwater potential zones and recommendation of artificial recharge structures for augmentation of groundwater resources in Vattamalaikarai Basin, South India. Environmental Earth Sciences, 79(5): 102. DOI：10.1007/s12665-020-8832-9.

Atmaja RRS, Putra DPE, Setijadji LD. 2019. Delineation of groundwater potential zones using remote sensing, GIS, and AHP techniques in southern region of Banjarnegara, Central Java, Indonesia. Sixth Geoinformation Science Symposium, 192-202. DOI：10.1117/12.2548473.

Berhanu KG, Hatiye SD. 2020. Identification of groundwater potential zones using proxy sata: Case study of Megech Watershed, Ethiopia. Journal of Hydrology: Regional Studies, 28(February): 100676. DOI：10.1016/j.ejrh.2020.100676.

Biswas S, Mukhopadhyay BP, Bera A. 2020. Delineating groundwater potential zones of agriculture dominated landscapes using GIS based AHP techniques: A case study from Uttar Dinajpur district, West Bengal. Environmental Earth Sciences, 79(12): 302. DOI：10.1007/s12665-020-09053-9.

Das B, Pal SC, Malik S, et al. 2019. Modeling groundwater potential zones of Puruliya district, West Bengal, India using remote sensing and GIS techniques. Geology, Ecology, and Landscapes, 3(3): 223−237. DOI：10.1080/24749508.2018.1555740.

Das S, Pardeshi SD. 2018. Integration of different influencing factors in GIS to delineate groundwater potential areas using IF and FR techniques: A study of Pravara basin, Maharashtra, India. Applied Water Science, 8(7):

1−16. DOI：10.1007/s13201-018-0848-x.

Deepa S, Venkateswaran S, Ayyandurai R, et al. 2016. Groundwater recharge potential zones mapping in upper Manimuktha Sub Basin Vellar River Tamil Nadu India using GIS and remote sensing techniques. Modeling Earth Systems and Environment, 2(3): 1−13. DOI：10.1007/s40808-016-0192-9.

Duan HJ, Deng ZD, Deng FF, et al. 2016. Assessment of groundwater potential based on multicriteria decision making model and decision tree algorithms. Mathematical Problems in Engineering, 2016: 1−12. DOI：10.1155/2016/2064575.

Ettazarini S, El Jakani M. 2020. Mapping of groundwater potentiality in fractured aquifers using remote sensing and GIS techniques: The case of Tafraoute region, Morocco. Environmental Earth Sciences, 79(5): 105. DOI：10.1007/s12665-020-8848-1.

Fildes SG, Clark IF, Somaratne NM, et al. 2020. Mapping groundwater potential zones using remote sensing and geographical information systems in a fractured rock setting, Southern Flinders Ranges, South Australia. Journal of Earth System Science, 129(1): 160. DOI：10.1007/s12040-020-01420-1.

Gelagay HS, Minale AS. 2016. Soil loss estimation using GIS and Remote sensing techniques: A case of Koga watershed, Northwestern Ethiopia. International Soil and Water Conservation Research, 4(2): 126−136. DOI：10.1016/j.iswcr.2016.01.002.

Hammouri N, El-naqa A, Barakat M. 2012. An integrated approach to groundwater exploration using remote sensing and geographic information system. Journal of Water Resource and Proteciton, 4(9): 717−724. DOI：10.4236/jwarp.2012.49081.

Haque SM, Kannaujiya S, Taloor AK, et al. 2020. Identification of groundwater resource zone in the active tectonic region of Himalaya through earth observatory techniques. Groundwater for Sustainable Development, 10: 100337. DOI：10.1016/j.gsd.2020.100337.

Ikegwuonu ES, Balogun DO, Agunloye O, et al. 2021. Geospatial assessment of groundwater potential in Jos south local government area of Plateau State, Nigeria. International Journanl of Engineering Research and Technology, 10(3): 27−38.

Jabbar FK, Grote K, Tucker RE. 2019. A novel approach for assessing watershed susceptibility using weighted overlay and analytical hierarchy process ( AHP ) methodology : A case study in Eagle Creek Watershed, USA. Environmental Science and Pollution Research, 26: 31981−31997. DOI：10.1007/s11356-019-06355-9.

Janarthanan G, Thirukumaran V. 2020. Mapping of groundwater potential zones in Pulampatti Watershed, Dharmapuri District – a geospatial approach. Indian Journal of Natural Sciences, 12(66): 1−9.

Kassahun N, Mohamed M. 2018. Groundwater potential assessment and characterization of Genale-Dawa River Basin. Open Journal of Modern Hydrology, 08(04): 126−144. DOI：10.4236/ojmh.2018.84010.

Kavidha R, Elangovan K. 2012. Assessment of groundwater potential zones in erode district, tamil nadu, by using gis techniques. Pollution Research, 31(2): 161−167.

Kindie AT, Enku T, Moges MA. 2019. Spatial analysis of groundwater potential using GIS based multi criteria dcision analysis method in Lake Tana Basin, Ethiopia (Vol. 2). International Conference on Advances of Science and Technology. Cham: Springer, 2019: 439−456. DOI：10.1007/978-3-030-15357-1_37.

Pande CB, Moharir KN, Panneerselvam B, et al. 2021. Delineation of groundwater potential zones for sustainable development and planning using analytical hierarchy process (AHP), and MIF techniques. Applied Water Science, 11(12): 1−20. DOI：10.1007/s13201-021-01522-1.

Province B, Kaewdum N, Chotpantarat S. 2021. Mapping potential zones for groundwater recharge using a GIS technique in the Lower Khwae Hanuman Sub-Basin area. Prachin, 9: 1−16. DOI：10.3389/feart.2021.717313.

Rajasekhar M, Sudarsana Raju G, Sreenivasulu Y, et al. 2019. Delineation of groundwater potential zones in semi-arid region of Jilledubanderu River Basin, Anantapur District, Andhra Pradesh, India using fuzzy logic, AHP and integrated fuzzy-AHP approaches. HydroRe-

search, 2: 97−108. DOI：10.1016/j.hydres.2019.11.006.

Saha A, Patil M, Karwariya S, et al. 2018. Identification of potential sites for water harvesting structures using geospatial techniques and multi-criteria decision analysis. The International Archives of the Photogrammetry, Remote Sensing and Spatial Information Science, XLII-5: 329−334. DOI：10.5194/ISPRS-ARCHIVES-XLII-5-329-2018.

Saranya T, Saravanan S. 2020. Groundwater potential zone mapping using analytical hierarchy process (AHP) and GIS for Kancheepuram District, Tamilnadu, India. Modeling Earth Systems and Environment, 6(2): 1105−1122. DOI：10.1007/s40808-020-00744-7.

Savita RS, Mittal HK, Satishkumar U, et al. 2018. Delineation of groundwater potential zones using remote sensing and GIS techniques in Kanakanala Reservoir Subwatershed, Karnataka, India. International Journal of Current Microbiology and Applied Sciences, 7(1): 273−288. DOI：10.20546/ijcmas.2018.701.030.

Shadeed SM, Judeh TG, Almasri MN. 2019. Developing GIS-based water poverty and rainwater harvesting suitability maps for domestic use in the Dead Sea region(West Bank, Palestine). Hydrogeology and Earth System Science, 23(3): 1581−1592. DOI：10.5194/hess-23-1581-2019.

Shao ZF, Huq ME, Cai BW, et al. 2020. Integrated remote sensing and GIS approach using Fuzzy-AHP to delineate and identify groundwater potential zones in semi-arid Shanxi Province, China. Environmental Modelling and Software, 134: 104868. DOI：10.1016/j.envsoft.2020.104868.

Sivakumar V, Vinay LY, Reddy K. 2019. Identification of groundwater potential zones using gis and remote sensing. International Journal of Pure and Applied Mathematics, 119(17): 3195-3210.

Suryabhagavan K. 2017. Application of remote sensing and GIS for groundwater potential zones identification in Bata river basin, Himachal Pradesh, India. Journal of Geomatics, 11(1): 66−76.

Takorabt HZS. et al. 2018. Determining the role of lineaments in underground hydrodynamics using Landsat 7 ETM + data, case of the Chott El Gharbi Basin (western Algeria). Arabian Journal of Geosciences, 11(4): 76. DOI：10.1007/s12517-018-3412-y.

Teja KS, Singh D. 2019. Identification of groundwater potential zones using remote sensing and GIS, case study: Mangalagiri mandal. International Journal of Recent Technology and Engineering, 7(6): 860−864.

Thapa R, Gupta S, Guin S, et al. 2018. Sensitivity analysis and mapping the potential groundwater vulnerability zones in Birbhum district, India: A comparative approach between vulnerability models. Water Science, 32(1): 44−66. DOI：10.1016/j.wsj.2018.02.003.

Yeh HF, Cheng YS, Lin HI, et al. 2016. Mapping groundwater recharge potential zone using a GIS approach in Hualian River, Taiwan. Sustainable Environment Research, 26(1): 33−43. DOI：10.1016/j.serj.2015.09.005.